

# *Studies concerning the growth of cadmium dendrites.*

## *II. Morphology in acidic media*

R. BARNARD, G. S. EDWARDS, J. HOLLOWAY, F. L. TYE

*Berec Group Limited, Group Technical Centre, St. Ann's Road, London N15 3TJ, UK*

Received 31 January 1983

The morphology of cadmium deposits formed during potentiostatic deposition onto etched cadmium substrates in a range of cadmium sulphate solutions with  $0.5 \text{ mol dm}^{-3}$  sulphuric acid as supporting electrolyte has been investigated. The deposit morphology and induction time was found to be both concentration and overpotential dependent. At  $10^{-1} \text{ mol dm}^{-3} \text{ CdSO}_4$  for an overpotential range  $-20$  to  $-80 \text{ mV}$ , large crystalline aggregates were observed and large dendrites resulted after longer deposition times. The induction time was less than 1 min and the current time curves linear, indicating instantaneous rather than progressive initiation. At  $10^{-2} \text{ mol dm}^{-3} \text{ CdSO}_4$  the morphology varied from fine, 2D-fern dendrites at  $\eta = -75 \text{ mV}$  to needle dendrites at  $\eta = -150 \text{ mV}$ . The morphology at  $10^{-3} \text{ mol dm}^{-3} \text{ CdSO}_4$  closely resembled that at  $10^{-2} \text{ mol dm}^{-3} \text{ CdSO}_4$  but, showed finer structural detail with less filling in of the main skeletal structure. The induction time was an order of magnitude greater at  $10^{-3} \text{ mol dm}^{-3} \text{ CdSO}_4$  than at  $10^{-2} \text{ mol dm}^{-3} \text{ CdSO}_4$ , and the time taken to grow dendrites of the same length was also increased.

### 1. Introduction

In the first part of this investigation [1] factors governing the growth of cadmium dendrites from alkaline solution were investigated. The alkaline system is, however, difficult to study fully because of the limited solubility of  $\text{Cd}(\text{OH})_4^{2-}$  ( $1.05 \times 10^{-4} \text{ mol dm}^{-3}$  in 30% KOH) and this factor precludes detailed study of important concentration dependences. It seems highly likely that the long induction time associated with the growth of cadmium dendrites is also related to the low concentration of  $\text{Cd}(\text{OH})_4^{2-}$ . The dendrite growth process may also be modified by the presence of suspended or colloidal  $\text{Cd}(\text{OH})_2$  in the electrolyte. Simultaneous evolution of hydrogen on nickel or cadmium substrates at high overpotentials needed to initiate dendrite growth is an added complication.

It was considered worthwhile therefore to study the growth of cadmium dendrites from acidic medium ( $\text{CdSO}_4/0.5 \text{ mol dm}^{-3} \text{ H}_2\text{SO}_4$ ) over a range of cadmium concentrations from  $10^{-1}$  to  $10^{-4} \text{ mol dm}^{-3}$ . By this means complications associated with the alkaline system can be circumvented and it is possible to more fully test

the various dendrite growth theories. This facilitates a better understanding of the growth of cadmium dendrites from alkaline solution. As will be shown later in Part III, it appears that the dendrite growth theories are equally applicable to both the acidic and alkaline supporting electrolyte cases.

The present investigation will be restricted to a discussion of the morphology of the dendrites obtained from  $\text{CdSO}_4/\text{H}_2\text{SO}_4$  solutions. These results will be used again in Part III.

### 2. Experimental procedure

Potentiostatic deposition of cadmium from  $\text{CdSO}_4/0.5 \text{ mol dm}^{-3} \text{ H}_2\text{SO}_4$  onto a stationary cadmium substrate was studied using the procedures described previously [1]. A range of  $\text{CdSO}_4$  concentrations from  $10^{-1}$  to  $10^{-4} \text{ mol dm}^{-3}$  were employed together with cadmium wire counter and reference electrodes. The polished cadmium wire ( $0.00785 \text{ cm}^2$ , cross-sectional area) was subjected to chemical etching (5 s in 50%  $\text{HNO}_3$ ) before use.

In the case of dilute  $\text{CdSO}_4$  solutions ( $< 10^{-2}$

$\text{mol dm}^{-3}$ ) it was important to remove the cadmium counter and reference electrodes from the cell when not in use because slight corrosion and dissolution of the cadmium electrodes over periods of a day could significantly change the concentration of the working solution. The concentrations of the working solutions were checked using atomic absorption spectrophotometry.

### 3. Results and discussion

#### 3.1. Potentiostatic current-time curves

Fig. 1 shows a family of current-time curves obtained at fixed overpotential of  $-150$  mV for the deposition of cadmium onto a stationary cadmium substrate from various concentrations of  $\text{CdSO}_4$  in  $0.5 \text{ mol dm}^{-3} \text{ H}_2\text{SO}_4$  supporting electrolyte. At the lowest  $\text{CdSO}_4$  concentration ( $10^{-4} \text{ mol dm}^{-3}$ ) following the initial decline in current, the latter parameter remains relatively constant over many hours of deposition. In the case of  $10^{-3} \text{ mol dm}^{-3} \text{ CdSO}_4$ , the current shows a slow rise after an induction time of about 60 min.

Increasing the  $\text{CdSO}_4$  concentration further to  $10^{-2} \text{ mol dm}^{-3}$  leads to a rapid rise in current after a short induction period of about 5 min. The parabolic dependence of current on time identified here is similar to that found previously [1] for the deposition of cadmium from 30% KOH containing  $1.05 \times 10^{-4} \text{ mol dm}^{-3} \text{ Cd(OH)}_4^{2-}$  at a rotating nickel disc electrode. The increase in current with time after the induction period arises from the gradually increasing surface area of the electrode deposit and may indicate the presence of dendrites.

The results of Fig. 1 illustrate the marked dependence of the shape of the potentiostatic current-time curves on the concentration of the depositing species. Furthermore, the induction period before the rise in current (or appearance of dendrites) is also inversely proportional to the concentration of the depositing species. Thus, at a concentration of  $10^{-4} \text{ mol dm}^{-3}$  for the same diffusional conditions, it would be inferred that at least 10 h would be required before a rise in current would be observed. Certainly dendrites were absent on the electrode surface after 8 h

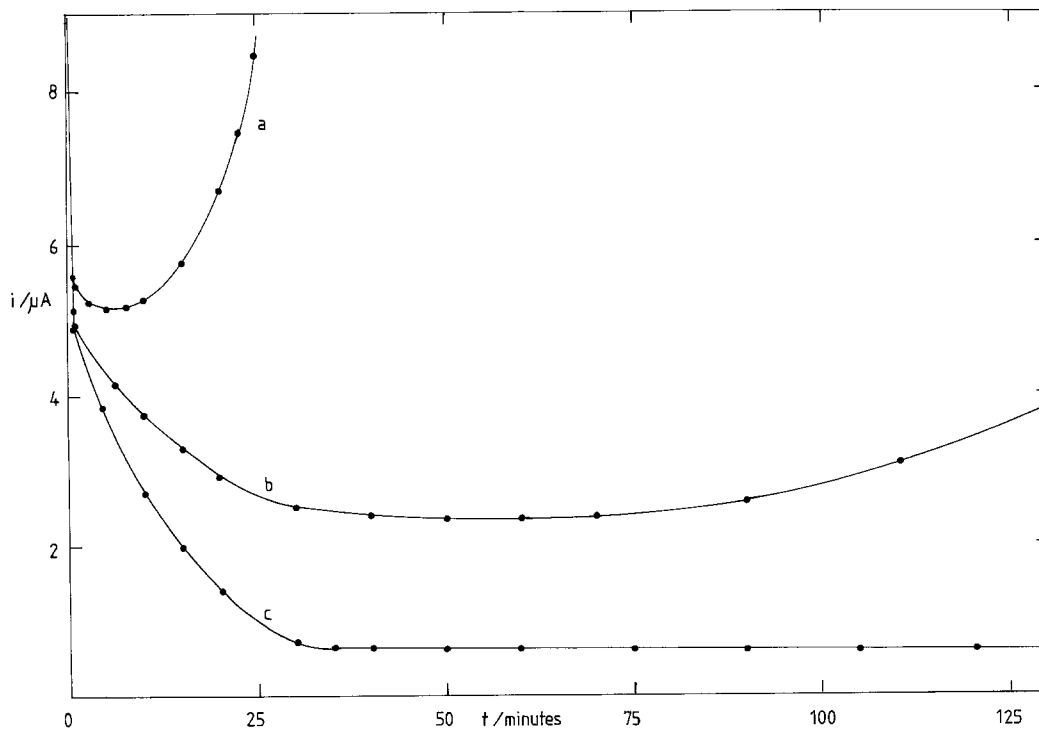


Fig. 1. Current-time curves for cadmium deposition at  $\eta = -150$  mV onto stationary cadmium substrates for various concentrations of  $\text{CdSO}_4$  in  $0.5 \text{ mol dm}^{-3} \text{ H}_2\text{SO}_4$  supporting electrolyte.  $a = 10^{-2} \text{ mol dm}^{-3}$ ;  $b = 10^{-3} \text{ mol dm}^{-3}$ ;  $c = 10^{-4} \text{ mol dm}^{-3}$ .

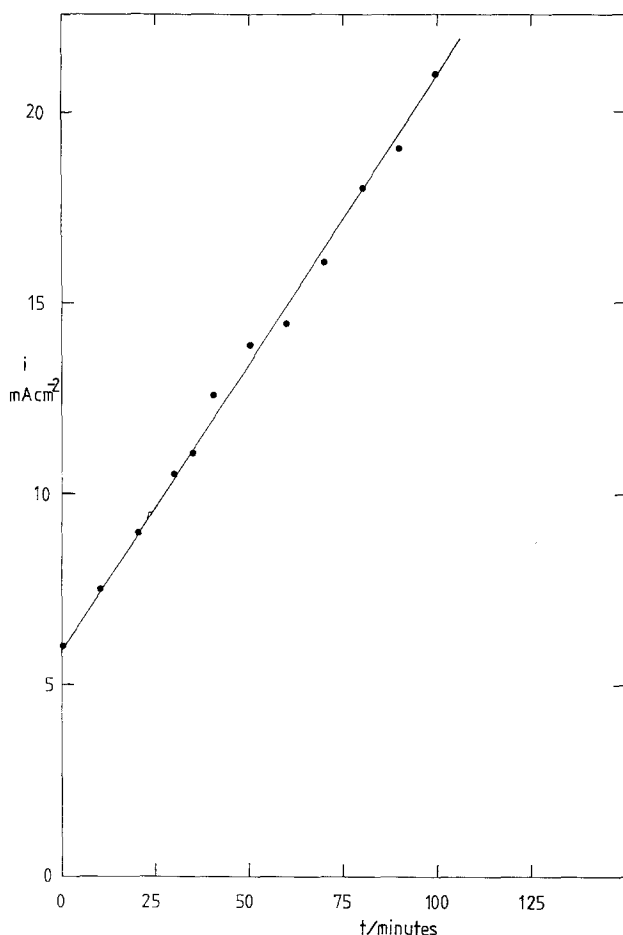


Fig. 2. Linear current density-time plot for cadmium deposition at  $\eta = -80$  mV onto a stationary cadmium substrate in  $10^{-1}$  mol dm<sup>-3</sup> CdSO<sub>4</sub>/0.5 mol dm<sup>-3</sup> H<sub>2</sub>SO<sub>4</sub>.

deposition periods, (but see Section 3.2.4). Conversely, at high CdSO<sub>4</sub> concentration ( $10^{-1}$  mol dm<sup>-3</sup>), the induction time is less than 1 min and the current rises rapidly in a linear fashion from the start of the experiment as shown in Fig. 2 for  $\eta = -80$  mV. This linear rise in current  $i$  with time  $t$  suggests that the dendrites are initiating instantaneously [2] rather than progressively ( $i \propto t^2$ ).

The current-time curves at fixed concentration of depositing metal ion are potential dependent as might be expected. Fig. 3 illustrates the current-time behaviour observed over a range of overpotentials  $\eta$  from  $-25$  to  $-150$  mV for  $10^{-2}$  mol dm<sup>-3</sup> CdSO<sub>4</sub>. At overpotentials below  $-150$  mV, the induction period is extended and the rise in current after induction less rapid.

Popov *et al.* [3] have similarly studied the growth of dendrites from  $10^{-1}$  mol dm<sup>-3</sup>

CdSO<sub>4</sub>/0.5 mol dm<sup>-3</sup> H<sub>2</sub>SO<sub>4</sub>. These workers found relationships where  $\log i \propto t$  after induction, the slope of the linear sections changing with overpotential ( $-60$  to  $-100$  mV). Popov *et al.* [3] claim induction periods of  $\sim 2$  min at  $\eta = -100$  mV for  $10^{-1}$  mol dm<sup>-3</sup> CdSO<sub>4</sub>. This induction time, although relatively small, is probably larger than might have been anticipated on the basis of the likely surface state of the electrodes used by Popov *et al.* Their electrodes were prepared by pre-electrodeposition of cadmium onto a platinum substrate and from the low magnification optical micrographs presented, considerable surface irregularity was clearly present from the onset of the dendrite growth experiments.

### 3.2. Morphology of electrodeposits

The morphologies and lengths of the dendrites

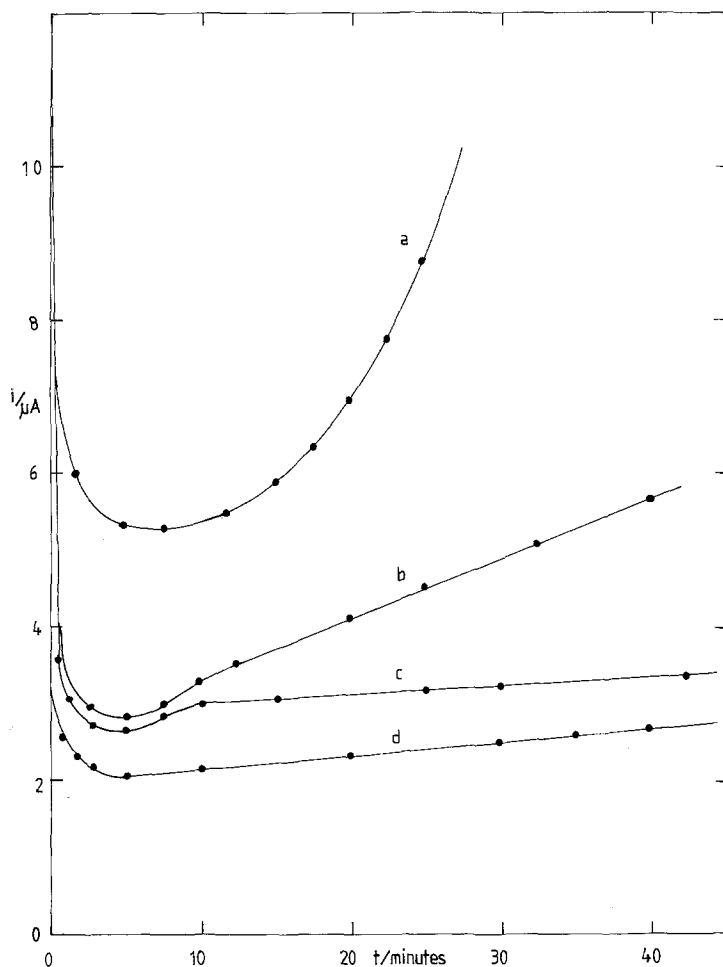


Fig. 3. Current-time curves for cadmium deposition onto stationary cadmium substrates in  $10^{-2}$  mol dm $^{-3}$  CdSO $_4$ /0.5 mol dm $^{-3}$  H $_2$ SO $_4$  for various overpotentials. (a) -150 mV; (b) -100 mV; (c) -50 mV; (d) -25 mV.

Table 1. Morphology and lengths of dendrites formed on stationary cadmium substrates in cadmium sulphate solutions in 0.5 mol dm $^{-3}$  H $_2$ SO $_4$  supporting electrolyte

Concentration of CdSO $_4$ (mol dm $^{-3}$ )	$\eta$ (mV)	Total deposition time (min)	Average dendrite length ( $\mu$ m)	Morphology
$10^{-1}$	-20	100	309	Crystalline aggregates
	-35	90	637	
	-80	20	2184	Dendrite
$10^{-2}$	-75	30	241	Ferns
	-100	27	300	Mixture of ferns and needles of similar length
	-150	35	333	Needles
$10^{-3}$	-100	300	78	Ferns
	-125	330	111	Ferns
	-150	130	205	Needles

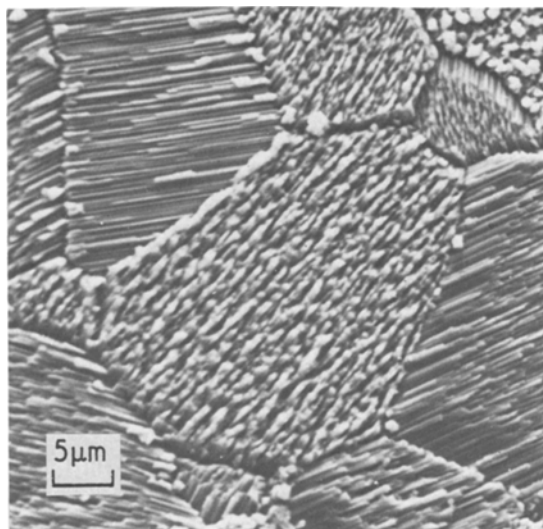


Fig. 4. Initial grain structure of etched cadmium substrate.

obtained from various  $\text{CdSO}_4$  concentrations over a range of overpotentials are summarized in Table 1.

In this series of experiments, a chemically etched cadmium substrate was employed as indicated in the experimental section. The initial grain structure of the cadmium surface after etching is shown in Fig. 4.

### 3.2.1. $10^{-1} \text{ mol dm}^{-3} \text{ CdSO}_4 / 0.5 \text{ mol dm}^{-3} \text{ H}_2\text{SO}_4$

Deposition of cadmium from  $10^{-1} \text{ mol dm}^{-3}$

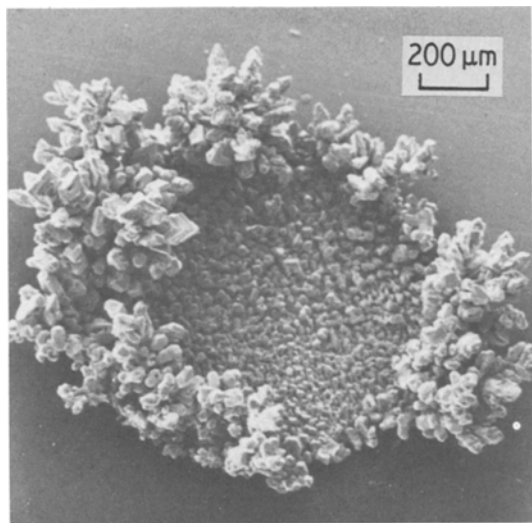


Fig. 5. Cadmium deposit on a stationary cadmium substrate after 20 minutes deposition at  $\eta = -80 \text{ mV}$  in  $10^{-1} \text{ mol dm}^{-3} \text{ CdSO}_4 / 0.5 \text{ mol dm}^{-3} \text{ H}_2\text{SO}_4$ . General view.

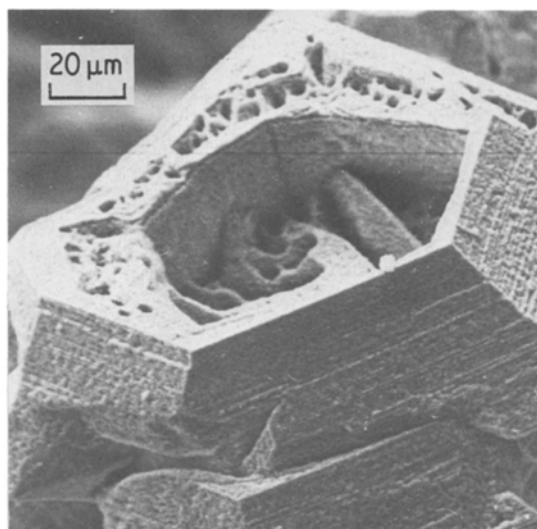


Fig. 6. Cadmium deposit on a stationary cadmium substrate after 20 minutes deposition at  $\eta = -80 \text{ mV}$  in  $10^{-1} \text{ mol dm}^{-3} \text{ CdSO}_4 / 0.5 \text{ mol dm}^{-3} \text{ H}_2\text{SO}_4$ . Higher magnification of part of Fig. 5.

$\text{CdSO}_4$  was very rapid and took place with negligible induction period. Fig. 5 shows the type of deposit observed after only 20 min at  $\eta = -80 \text{ mV}$ . Deposition is observed to take place predominantly at the edge of the electrode on the boundary between the cadmium substrate and the moulding material with the formation of a ring of crystalline aggregates. Fig. 6 shows the deposits at higher magnification.

A common and characteristic feature of these deposits, clearly illustrated in Fig. 6, was the presence of hexagonal holes. These holes are thought to arise from defects in the crystal structure which have been replicated and amplified.

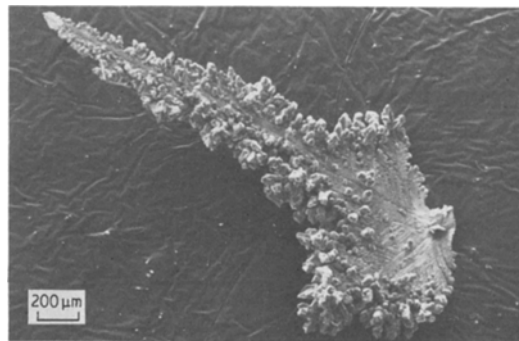


Fig. 7. Cadmium dendrite formed on a stationary cadmium substrate at  $\eta = -80 \text{ mV}$  in  $10^{-1} \text{ mol dm}^{-3} \text{ CdSO}_4 / 0.5 \text{ mol dm}^{-3} \text{ H}_2\text{SO}_4$ . General view.

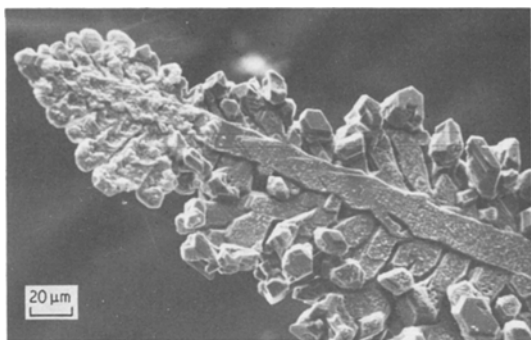


Fig. 8. Cadmium dendrite formed on a stationary cadmium substrate at  $\eta = -80$  mV in  $10^{-1}$  mol dm $^{-3}$  CdSO $_4$ /0.5 mol dm $^{-3}$  H $_2$ SO $_4$ . Higher magnification of Fig. 7.

Their origin probably lies in several lattice sites being simultaneously devoid of atoms as a consequence of blockage by impurities in the initial stages of lattice replication. Such hexagonal holes can be predicted from a Monte Carlo simulation of the growth process [4].

If the deposition is continued at  $\eta = -80$  mV then large dendrites can result. Fig. 7 shows a dendrite (> 2 mm long) which became detached from the electrode surface and was mounted separately for SEM examination. Fig. 8 shows the tip of the large dendrite of Fig. 7 in more detail. The main stalk and primary branches of the dendrite can be identified. Fig. 9 at still higher magnification, reveals that the outer parts of the branches and tip display the familiar stacking of hexagonal cadmium platelets [1].

**3.2.2.  $10^{-2}$  mol dm $^{-3}$  CdSO $_4$ /0.5 mol dm $^{-3}$  H $_2$ SO $_4$**   
At this lower concentration, the dendrites obtained

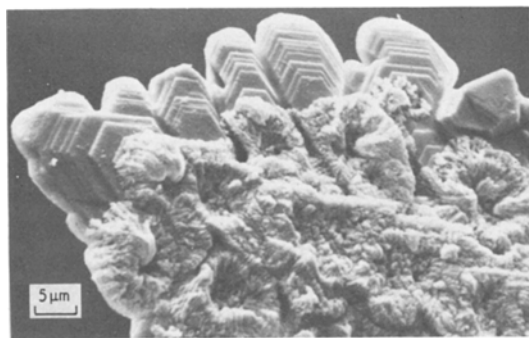


Fig. 9. Cadmium dendrite formed on a stationary cadmium substrate at  $\eta = -80$  mV in  $10^{-1}$  mol dm $^{-3}$  CdSO $_4$ /0.5 mol dm $^{-3}$  H $_2$ SO $_4$ . Dendrite tip at higher magnification.

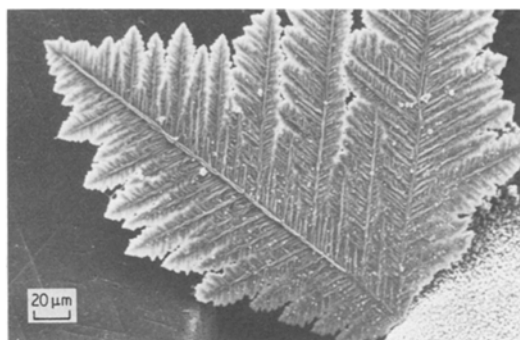


Fig. 10. Fern dendrites formed on a stationary cadmium substrate in  $10^{-2}$  mol dm $^{-3}$  CdSO $_4$ /0.5 mol dm $^{-3}$  H $_2$ SO $_4$  at  $\eta = -75$  mV. Well developed fern after 60 min deposition.

were noticeably of a more delicate texture and grow more slowly than at  $10^{-1}$  mol dm $^{-3}$  CdSO $_4$ . At low overpotentials  $\eta = -75$  mV the dendrites obtained had a thin, almost 2-dimensional, fern-like morphology as illustrated in Figs. 10 and 11. The thinness of the dendrites can be judged from the bottom right-hand corner of Fig. 11 where two dendrites can be seen 'edge-on'. At higher overpotentials the dendrites tend towards a needle-like morphology as can be seen from Figs. 12 and 13 at  $\eta = -150$  mV. The curious flake like outgrowths on the needle branches (Fig. 13) may, perhaps, indicate a tendency to revert to the fern morphology at higher values of  $\eta$ . A mixture of needle and fern-like dendrites can be observed at intermediate overpotentials,  $\eta = -100$  mV as shown in Fig. 14.

**3.2.3.  $10^{-3}$  mol dm $^{-3}$  CdSO $_4$ /0.5 mol dm $^{-3}$  H $_2$ SO $_4$**   
Dendrites obtained at  $10^{-3}$  mol dm $^{-3}$  CdSO $_4$

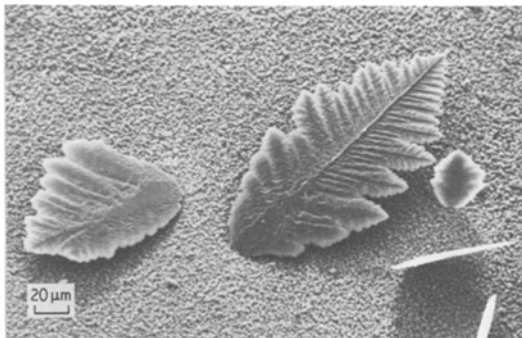


Fig. 11. Fern dendrites formed on a stationary cadmium substrate in  $10^{-2}$  mol dm $^{-3}$  CdSO $_4$ /0.5 mol dm $^{-3}$  H $_2$ SO $_4$  at  $\eta = -75$  mV. Small thin ferns and electrode back-ground showing dendrite precursors.

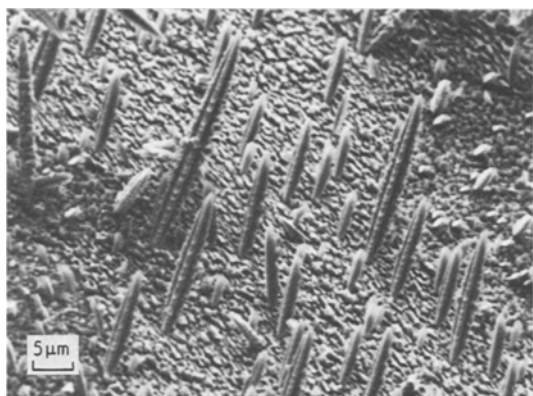


Fig. 12. Dendrites formed on a stationary cadmium substrate in  $10^{-2} \text{ mol dm}^{-3} \text{ CdSO}_4/0.5 \text{ mol dm}^{-3} \text{ H}_2\text{SO}_4$ . Needle dendrites formed after 35 min at  $\eta = -150 \text{ mV}$ .

closely resembled those obtained at  $10^{-2} \text{ mol dm}^{-3} \text{ CdSO}_4$ . The induction time before the dendrites appear is an order to magnitude greater than at  $10^{-2} \text{ mol dm}^{-3}$ . This aspect has already been discussed in Section 3.1.

The time taken to reach the same dendrite length is increased at  $10^{-3} \text{ mol dm}^{-3}$  compared to  $10^{-2} \text{ mol dm}^{-3} \text{ CdSO}_4$  as might be expected. Dendrites grown at this lower concentration show finer structural detail owing to less 'filling-in' of the main sketched structure. At lower overpotentials, ( $\eta = -80 \text{ mV}$ ) fern-like dendrites are observed as in Fig. 15 whilst at higher overpotentials ( $\eta = -150 \text{ mV}$ ) a change-over to needle-like dendrites results as in Fig. 16. This type of behaviour is similar to that already discussed con-

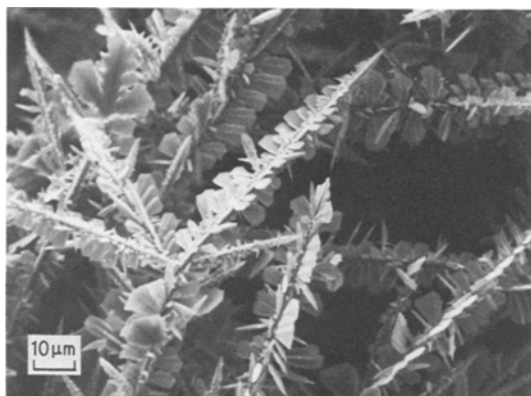


Fig. 13. Dendrites formed on a stationary cadmium substrate in  $10^{-2} \text{ mol dm}^{-3} \text{ CdSO}_4/0.5 \text{ mol dm}^{-3} \text{ H}_2\text{SO}_4$ . Needle dendrites with flake growth on the branches formed after 35 min at  $\eta = -150 \text{ mV}$ .

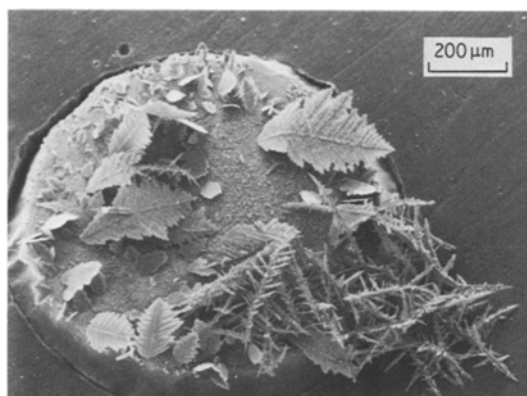


Fig. 14. Dendrites formed on a stationary cadmium substrate in  $10^{-2} \text{ mol dm}^{-3} \text{ CdSO}_4/0.5 \text{ mol dm}^{-3} \text{ H}_2\text{SO}_4$ . Mixture of fern and needle dendrites formed after 27 min at  $\eta = -100 \text{ mV}$ .

cerning the growth of dendrites in alkaline media in Part I [1].

Fig. 17 shows a mat of dendrites formed after 60 min deposition at  $\eta = -150 \text{ mV}$ . These needle-like dendrites closely resemble those obtained [1] after extensive deposition from alka-

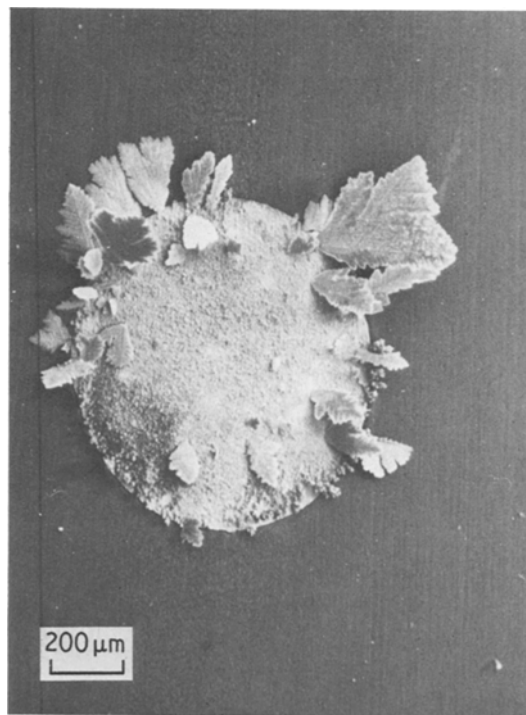


Fig. 15. Cadmium deposits formed on a stationary cadmium substrate in  $10^{-3} \text{ mol dm}^{-3} \text{ CdSO}_4/0.5 \text{ mol dm}^{-3} \text{ H}_2\text{SO}_4$ . Fern dendrites formed after 80 min at  $\eta = -80 \text{ mV}$ .

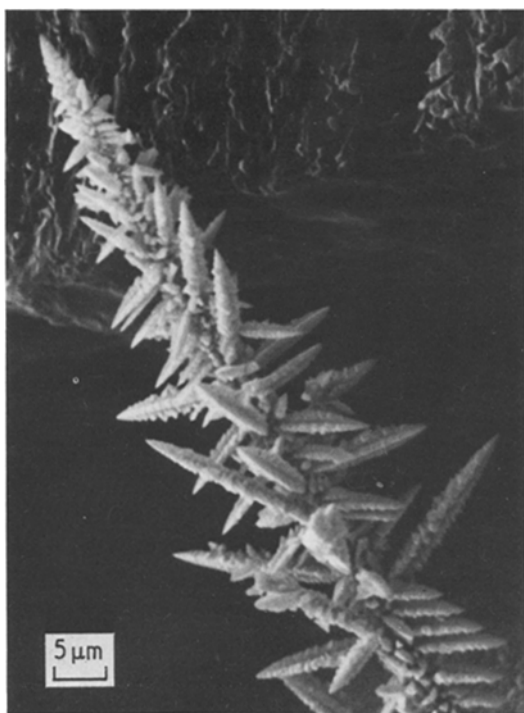


Fig. 16. Cadmium deposits formed on a stationary cadmium substrate in  $10^{-3} \text{ mol dm}^{-3} \text{ CdSO}_4/0.5 \text{ mol dm}^{-3} \text{ H}_2\text{SO}_4$ . Needle dendrites formed after 120 min at  $\eta = -150 \text{ mV}$ .

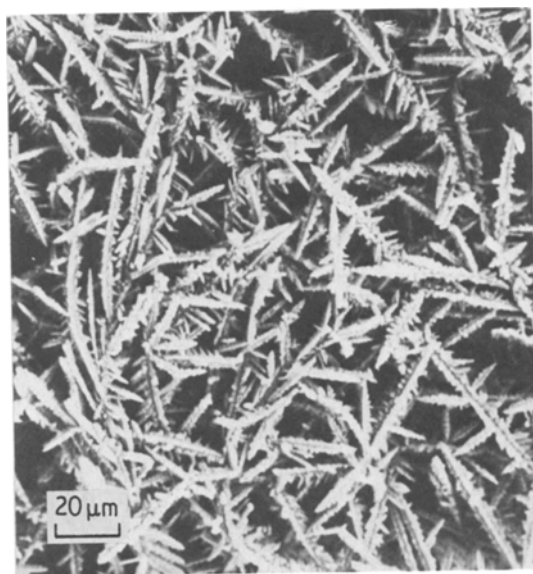


Fig. 17. Cadmium deposits formed on a stationary cadmium substrate in  $10^{-3} \text{ mol dm}^{-3} \text{ CdSO}_4/0.5 \text{ mol dm}^{-3} \text{ H}_2\text{SO}_4$ . Mat of needle dendrites formed after 60 min at  $\eta = -150 \text{ mV}$ .

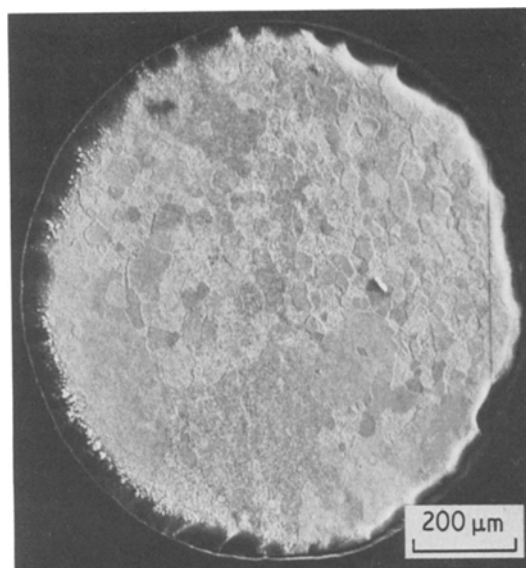


Fig. 18. Cadmium deposits formed on a stationary cadmium substrate in  $10^{-3} \text{ mol dm}^{-3} \text{ CdSO}_4/0.5 \text{ mol dm}^{-3} \text{ H}_2\text{SO}_4$ . Overlapping flake deposit formed after 400 min at  $\eta = -250 \text{ mV}$ .

line media ( $2.4 \times 10^{-4} \text{ mol dm}^{-3} \text{ Cd}(\text{OH})_4^{2-}/50\% \text{ KOH}$ ).

At the highest overpotentials ( $\eta = -200 \text{ mV}$ ) a relatively compact cadmium deposit can be obtained which, on closer examination, consists of layers of overlapping flakes (see Fig. 18).

**3.2.4.  $10^{-4} \text{ mol dm}^{-3} \text{ CdSO}_4/0.5 \text{ mol dm}^{-3} \text{ H}_2\text{SO}_4$**   
Electrodes examined after deposition periods up to 45 h at  $\eta = -150 \text{ mV}$  showed surprisingly no evidence of cadmium deposit. The electrode retained the appearance of the etched surface shown previously in Fig. 4.

This effect is considered to be partly a consequence of the low concentration of deposition metal ion, but the rate of dendrite growth appears to be slower than that found previously for deposition of cadmium onto a stationary cadmium substrate using  $30\% \text{ KOH}/1.05 \times 10^{-4} \text{ mol dm}^{-3} \text{ Cd}(\text{OH})_4^{2-}$ . A possible explanation for the greater rate of dendrite growth in the earlier experiments might be attributed to suspended  $\text{Cd}(\text{OH})_2$  in the alkali leading to higher localized concentrations. Such complications are absent using  $0.5 \text{ mol dm}^{-3} \text{ H}_2\text{SO}_4$  supporting electrolyte.

A further and a more likely explanation may be ascribed to the redissolution of the reactive cadmium into the  $0.5 \text{ mol dm}^{-3} \text{ H}_2\text{SO}_4$  supporting



electrolyte immediately after deposition. It was noted previously that slow corrosion of the pure cadmium wire took place on open circuit in  $0.5 \text{ mol dm}^{-3} \text{ H}_2\text{SO}_4$  (note precautions in Experimental Section). It is possible that only a balance between the cathodic deposition and anodic corrosion rate was reached using the very low  $\text{CdSO}_4$  concentrations ( $\sim 10^{-4} \text{ mol dm}^{-3}$ ), even at  $\eta = -150 \text{ mV}$ .

#### 4. Conclusions

This study has revealed close similarities between the factors influencing cadmium dendrite growth from both alkaline and acidic supporting electrolytes.

The results indicate that the induction time associated with dendrite growth is both potential and concentration dependent. Induction time is approximately inversely proportional to the concentration of the depositing cadmium species (e.g.  $\sim 1 \text{ h}$  at  $10^{-3} \text{ mol dm}^{-3} \text{ CdSO}_4$  for  $\eta = -150 \text{ mV}$ ). Propagation rates for dendrites are similarly concentration dependent.

Dendrites produced at low overpotential from  $\text{CdSO}_4/\text{H}_2\text{SO}_4$  tend towards a thin 2-D fern-like texture whilst those at higher overpotentials display a needle-like morphology. At still higher overpotentials curious flake-like outgrowths appear on the needle-branches. Mixed growth types can be observed at intermediate potentials.

Dendrites grow rapidly from  $10^{-1} \text{ mol dm}^{-3} \text{ CdSO}_4/0.5 \text{ mol dm}^{-3} \text{ H}_2\text{SO}_4$  electrolyte and to a considerable length ( $> 2 \text{ mm}$  after 0.5 h). The deposits frequently display characteristic hexagonal-holes due to replication of crystal defects. Dendrites produced at lower  $\text{CdSO}_4$  concentration ( $10^{-2}$  or  $10^{-3} \text{ mol dm}^{-3}$ ) display a more delicate and less intergrown texture compared to the substantial crystalline aggregates or dendrites developed from the higher concentrations.

#### Acknowledgements

The authors thank the Directors of Berc Group Limited for permission to publish this work. The authors are also indebted to Dr R. D. Armstrong and Mr S. Churchouse of the University of Newcastle for many helpful discussions. Thanks are also due to Mr D. J. Buckle for assistance with scanning electron microscopy.

#### References

- [1] R. Barnard, J. Holloway, G. S. Edwards and F. L. Tye, *J. Appl. Electrochem.* **13** (1983) 000.
- [2] J. W. Diggle, A. R. Despic and J. O'M. Bockris, *J. Electrochem. Soc.* **116** (1969) 1503.
- [3] K. I. Popov, M. D. Maksimovic and J. D. Trnjancev, *J. Appl. Electrochem.* **11** (1981) 239.
- [4] R. D. Armstrong and S. Churchouse, private communication.